ChemComm

Accepted Manuscript

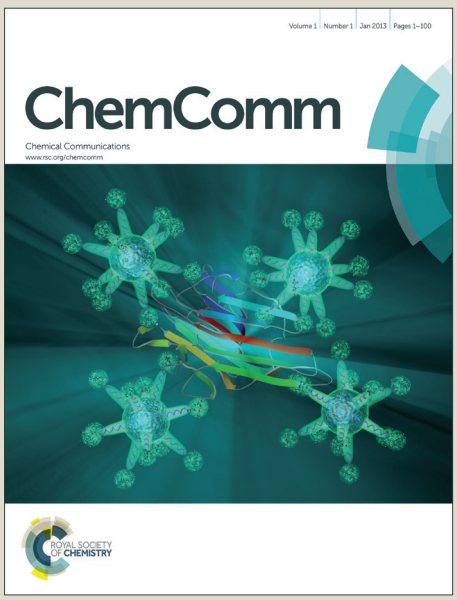

ROYAL SOCIETY OF CHEMISTRY

www.rsc.org/chemcomm

Cite this: DOI: 10.1039/c0xx00000x

www.rsc.org/xxxxxx

ARTICLE TYPE

Self-assembly of metal-organic coordination networks using on-surface synthesized ligands

Tao Lin,[a] Guowen Kuang,[a] Xue Song Shang,[b] Pei Nian Liu*[b] and Nian Lin*[a]

Received (in XXX, XXX) Xth XXXXXXXXX 20XX, Accepted Xth XXXXXXXXX 20XX

DOI: 10.1039/b000000x

Supramolecular assembly and on-surface synthesis are two widely-used methods for constructing low-dimensional molecular nanostructures on surface. Here we describe an approach that combines both methods to create two-dimensional metal-organic networks with exceptionally large pores.

Porous metal-organic framework (MOF) structures have attracted much attention because of their large surface area and capacity to store gases.[1] Significant effort has been made aiming for enlarging MOFs' pores. The largest pore so far recorded in MOFs is hexagonal one with an aperture up to 9.8 nm.[2] Two-dimensional (2D) MOF structures containing 2D pores can be fabricated on surfaces.[4] The largest 2D pore so far reported is of a hexagonal network assembled on a Ag(111) surface with a size of 24 nm^2.[5] Making larger pores requires longer organic ligands and/or multiple-component systems. However, synthesis of longer organic ligands usually encounters difficulties in purification due to their poor solubility. On the other hand, sublimation of longer ligands usually requires higher temperature, which may cause decomposition of the organic species. Both factors limit the size of the 2D porous MOFs.

Here we report a two-step strategy to overcome this limitation (Scheme 1). In the first step, we employ on-surface synthesis to covalently link a brominated terpyridyl ligand **1** to itself to form a bisterpyrydyl ligand **3** via Ullmann coupling; in the second step, **3** and a pyridyl-functionalized porphyrin compound **2** self-assemble via pyridyl-Fe-terpyridyl coordination into a porous network. Both steps take place in vacuo on an Au(111) surface. We can monitor the coupling reaction and self-assembly process using scanning tunneling microscopy (STM). In our experiments, we identified two types of 2D porous networks: irregularly-arranged Kagome networks with ~55 nm^2 pores and regular rhombus networks with ~22 nm^2 pores. Our results demonstrate a new route towards fabricating surface-supported 2D MOF structures with large pores.[6]

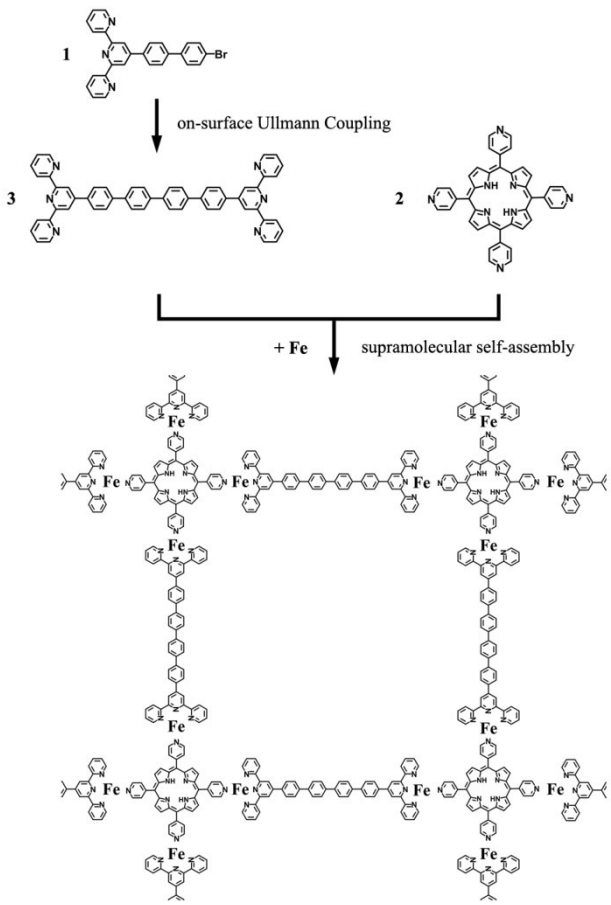

Scheme 1. Two-step process : (1) on-surface Ullmann coupling of **1** with itself to form **3,** and (2) self-assembly of **3** and **2** together with Fe to form a porous metal-organic network.

Fig. 1a is an STM topograph taken after deposition of compound **1** molecules on the surface; the image shows cluster-like features at the elbow positions of the herringbone reconstruction of the Au(111) surface. Most clusters look like a dog paw print, with four fingers attached to a base, which is clearly resolved in Fig. 1b. The clusters are ~2.0 nm wide, slightly longer than the 1.6-nm long molecule of **1**, but much shorter than the 2.88-nm long molecule of **3**. We conclude that the clusters are made of **1**. However, we are unable to build a realistic model for the "cluster" out of four molecules. Therefore we speculate that the dog paw print is associated with rotation of

a single molecule **1** on the surface at the experimental temperature (78 K).[6] The model shown in Fig. 1b illustrates how a molecule adopting four orientations separated by a rotation angle of approximately 40° generates the paw print pattern. Besides the objects adsorbed at herringbone elbows and at step edges, an appreciable amount of molecules moved very fast and were present on the open terrace in the 2D gas phase, which were not resolved by STM (see discussion below).

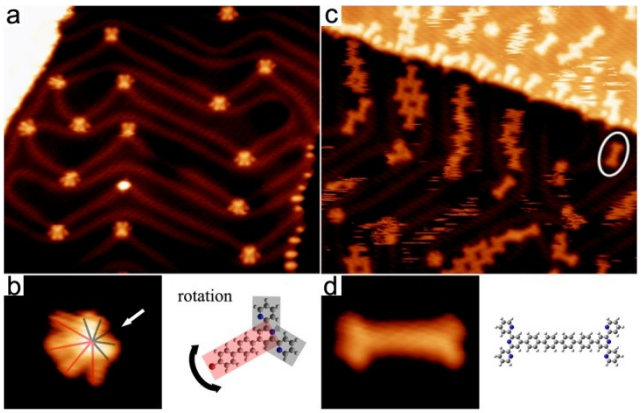

Fig. 1 (a) STM image (47 × 40 nm^2) showing **1** adsorbed on an Au(111) substrate. (b) High-resolution STM image (3.8 × 3.2 nm^2) and structural model of the dog paw print cluster. (c) STM image (47 × 40 nm^2) showing the sample after annealing at 150 °C for 5 minutes. The ellipse encloses a single molecule of **3**. (d) High-resolution STM image (3.8 × 3.2 nm^2) of a single molecule of **3** and the structural model.

Thermal annealing was applied to the sample in order to trigger Ullmann coupling at the terminal Br. After 5-min annealing at 180 °C, species shaped like a dog bone appeared on the surface. The ellipse in Fig. 1c encloses a single "dog bone" and Fig. 1d shows a high-magnification image. The dog-bone shape agrees well with the molecular structure of **3** (Fig. 1d), and its length (2.93 ± 0.06 nm) matches the length of **3** (2.88 nm). Thus, we conclude that Ullmann coupling occurred and two molecules of **1** were covalently linked to form the bis-terpyridyl compound **3**.[7] Apart from a few isolated molecules of **3,** most molecules packed in a shoulder-to-shoulder arrangement. It is known that the two side pyridyl groups in an un-coordinated terpyridyl group point backwardly.[8, 9] This conformation allows intermolecular hydrogen bonds between the terpyridyl groups in the shoulder-to-shoulder arrangement.[10] Further annealing at 180 °C for 15 min resulted in more dog-bone species, indicating that many "STM-invisible" fast-moving molecules of **1** had been converted to **3**. Note that terpyridyl ligand is well known to form complexes with Fe atoms.[11] We found that mixing **3** with Fe atoms on the surface formed coordination chains,[12] details see ESI.

In the next step, we deposited compound **2** and Fe atoms onto the sample and annealed it at 180 °C. Extended 2D porous networks were observed (Fig. 2a). Note that this network structure was never observed in the absence of Fe. The networks have rhombus geometry, occupying entire terraces and exhibiting three orientations with respect to the Au(111) substrate lattice. High-resolution STM reveals detailed characteristics of the network structure (Fig. 2b). The apex angle of the rhombus pore is 75° and the side length of the pore is 4.76 ± 0.03 nm. The long axis of the rhombus pores follows the <$\bar{1}$10> axis and equivalent directions of the Au(111) surface. The ideal network presented in Scheme 1 is of perfect square symmetry but the actual network shown in Fig. 2 is rhombus. The driving force for this distortion is symmetry mismatch between the ideal square network and the three-fold Au(111) substrate lattice. As the total energy of the surface-supported structures is contributed by intermolecular binding energy and molecule-substrate binding energy,[4] ideal structures are very often distorted to balance the energy cost due to symmetry mismatch. A similar phenomenon was observed before.[13]

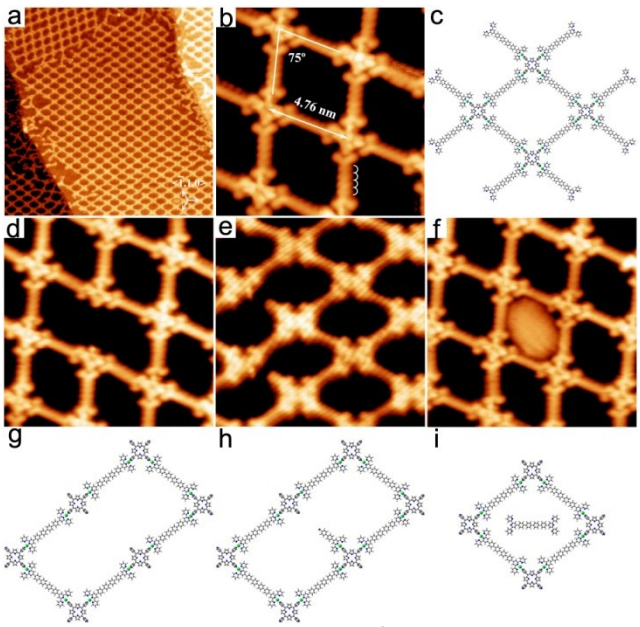

Fig. 2 (a) STM image (100 × 100 nm^2) showing porous rhombic networks. (b) High-resolution STM image (12 × 12 nm^2) of the rhombic networks. The wavy line indicates the phenyl rings in the backbone of **3**. (c) Tentative model of the rhombic network. (d), (e), (g) and (h) STM topographs (15 ×15 nm^2) showing two types of defects and the corresponding structural models (f) STM image (15 ×15 nm^2) showing a rhombic pore filled with guest species and (i) a suggested model of a guest molecule **3**.

The sub-molecular resolution in Fig. 2b allows us to determine that each pore is bordered by four molecules of **3,** which are connected by molecules of **2** at the four corners. Some molecules of **2** exhibit a depression at the center while others exhibit a protrusion at the center. The species with center depression are attributed to free-base porphyrin and those with center protrusion to Fe-metallated porphyrin.[14] The molecules **3** exhibit a four-node backbone (see the white wavy line in Fig. 2b), corresponding to the four phenyl rings of **3**. Four molecules of **3** attach to the four terminal pyridyl groups of a molecule **2** via the terpyridyl ligands. This structural motif is identical to the previously reported network formed from **2** and a shorter bis-terpyridyl ligand, 4′,4‴′-(1,4- phenylene)bis(2,2′:6′,2″-terpyridine), via pyridyl-Fe-terpyridyl coordination.[13] A structural model of the network is shown in Fig. 2c. The Fe-N bond is approximately 0.17 nm, assuming that both atoms lie in the same plane.[13] The model agrees well with the STM data. The pore area is ~22 nm^2, which is twice the size of previously-reported rhombic network.[13]

We observed two types of structural defects in the networks.

One is missing a linker molecule in the network, which leads to a double-size pore (Fig. 2d). The other is a molecule of **1** acting as a linker instead of **3,** resulting in two neighboring pores that are half-separated (Fig. 2e). The corresponding structural models of these defects are shown in Fig. 2g and 2h. It is worth to note that these defects are very rare, implying that both the Ullmann reaction and the metal-coordination assembly were very efficient. We also observed that pores were filled by guests (Fig. 2f). The cloud-like appearance of these guests resulted from rotating or oscillating molecules trapped in the pore at 78 K.[7, 13] The guests were most likely to be molecules of **1**, **2** or **3**. For example, Fig. 2i shows a tentative model of molecule **3** trapped in a pore.

Besides the extended regular rhombus networks, we also observed that small amount of molecules formed irregular networks featuring larger pores. Fig. 3a shows a network containing triangular and hexagonal pores. This structure resembles the Kagome network reported before.[13] The structural model of a Kagome unit is shown in Fig. 3b, in which **2** and **3** are linked by the same terpy-Fe-py coordination. The aperture of the hexagonal pore is 9.2 nm, and the pore area is ~55 nm^2. Both values are the largest ever reported for 2D MOF pores, and the aperure measures close to the current record (9.8 nm) for MOFs.[2] Unlike the previous work,[13] we did not observe a regular Kagome network of large domain size. It was shown that the rhombus structure can be converted into the Kagome structure when guest species expand the smaller rhombic pores into the larger Kagome pores. [13] Here the molecules of **1**, **2** and **3** are apparently not large enough to force this pore expansion (cf. Fig. 2i), which might be a reason that extended Kagome networks did not form. Nevertheless other mechanisms might play roles.

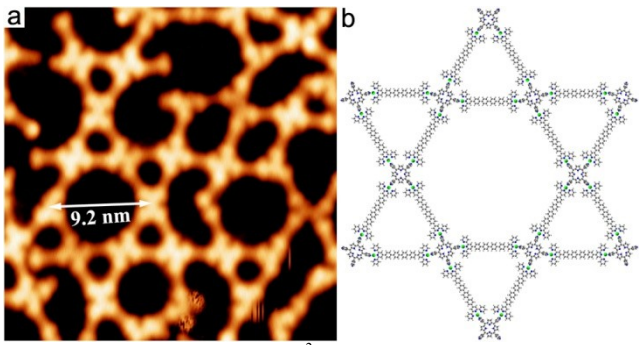

Fig. 3 (a) STM image (30 × 30 nm^2) of a defective Kagome network. (b) Structural model of the Kagome network.

In summary, we have demonstrated a two-step strategy to fabricate porous 2D metal-organic networks with large pores on an Au(111) surface. The first step involves obtaining large ligands via on-surface Ullmann coupling, followed by coordination self-assembly. Using STM, we monitored coupling and self-assembly, as well as resolving the porous structures and their defects. We believe that our protocol may provide new approach to design novel porous structures on surfaces.

This work is supported by Hong Kong RGC 602712, NSFC/China, the Basic Research Program of the Shanghai Committee of Sci. & Tech. (13NM1400802) and the Fundamental Research Funds for the Central Universities.

Notes and references

[a] *Department of Physics, The Hong Kong University of Science and Technology, Clear Water Bay, Hong Kong, China*
E-mail: phnlin@ust.hk
[b] *Shanghai Key Laboratory of Functional Materials Chemistry, Key Lab for Advanced Materials and Institute of Fine Chemicals, East China University of Science and Technology, Meilong Road 130, Shanghai, China*
E-mail: liupn@ecust.edu.cn

1 (a) O. M. Yaghi, M. O'Keeffe, N. W. Ockwig, H. K. Chae, M. Eddaoudi and J. Kim, *Nature*, 2003, **423**, 705; (b) S. Kitagawa, R. Kitaura and S. Noro, *Angew. Chem., Int. Ed.*, 2004, **43**, 2334; (c) H. Furukawa, K. E. Cordova, M. O'Keeffe and O. M. Yaghi, *Science*, 2013, **341**, 1230444.
2 H. Deng, S. Grunder, K. E. Cordova, C. Valente, H. Furukawa, M. Hmadeh, F. Gándara, A. C. Whalley, Z. Liu, S. Asahina, H. Kazumori, M. O'Keeffe, O. Terasaki, J. F. Stoddart and O. M. Yaghi, *Science*, 2012, **336**, 1018.
3 (a) S. De Feyter and F. C. De Schryver, *Chem. Soc. Rev.*, 2003, **32**, 139; (b) S. De Feyter and F. C. De Schryver, *J. Phys. Chem. B*, 2005, **109**, 4290; (c) C. A. Palma, M. Cecchini and P. Samorì, *Chem. Soc. Rev.*, 2012, **41**, 3713.
4 (a) J. V. Barth, *Annu. Rev. Phys. Chem.*, 2007, **58**, 375; (b) S. Stepanow, N. Lin and J. V. Barth, *J. Phys.: Condens. Matter*, 2008, **20**, 184002; (c) N. Lin, S. Stepanow, M. Ruben and J. V. Barth, *Top. Curr. Chem.*, 2009, **287**, 1; (d) L. Bartels, *Nat. Chem.*, 2010, **2**, 87; (e) H. Liang, Y. He, Y. Ye, X. Xu, F. Cheng, W. Sun, X. Shao, Y. Wang, J. Li and K. Wu, *Coord. Chem. Rev.*, 2009, **253**, 2959; (f) T. Kudernac, S. B. Lei, J. A. A. W. Elemans and S. De Feyter, *Chem. Soc. Rev.*, 2009, **38**, 402.
5 D. Kühne, F. Klappenberger, R. Decker, U. Schlickum, H. Brune, S. Klyatskaya, M. Ruben and J. V. Barth, *J. Am. Chem. Soc.*, 2009, **131**, 3881.
6 (a) J. K. Gimzewski, C. Joachim, R. R. Schlittler, V. Langlais, H. Tang and I. Johannsen, *Science*, 1998, **281**, 531; (b) L. Gao, Q. Liu, Y. Y. Zhang, N. Jiang, H. G. Zhang, Z. H. Cheng, W. F. Qiu, S. X. Du, Y. Q. Liu, W. A. Hofer and H.-J. Gao, *Phys. Rev. Lett.*, 2008, **101**, 197209; (c) D. Lensen and J. A. A. W. Elemans**,** *Chem. Soc. Rev*. 2012, **8**, 9053; (d) H. L. Tierney, J. W. Han, A. D. Jewell, E. V. Iski, A. E. Baber, D. S. Sholl and E. C. H. Sykes, *J. Phys. Chem. C*, 2011, **115**, 897.
7 (a) L. Grill, M. Dyer, L. Lafferentz, M. Persson, M. V. Peters, S. Hecht, *Nature Nanotechn.* 2007, **2**, 687; (b) J. Méndez, M. F. Lopez and J. A. Martín-Gago, *Chem. Soc. Rev*. 2011, **40**, 4578; (c) M. E. Garah, J. M. MacLeod, F. Rosei, *Surf. Sci.* 2013, **613**, 6; (d) G. Franc, A. Gourdon, *Phys.Chem.Chem.Phys.* 2011, **13**, 32, 14283; (e) M. Lackinger and W. M. Heckl, *J. Phys. D. Appl. Phy.* 2011, **44**, 46, 464011.
8 W. Wang, X. Shi, C. Lin, R. Q. Zhang, C. Minot, M. Van Hove, Y. Hong, B. Z. Tang, N. Lin, *Phys. Rev. Lett.* 2010, **105**, 126801.
9 A. Wild, A. Winter, F. Schlütter, U. S. Schubert, *Chem. Soc. Rev*. 2011, **40**, 1459.
10 W. Wang, S. Wang, Y. Hong, B. Z. Tang and N. Lin, *Chem. Commun.*, 2011, **47**, 10073.
11 T. Bauer**,** Z. Zheng, A. Renn, R. Enning, A. Stemmer, J. Sakamoto, A. D. Schlüter *Angew. Chem. Int. Ed*. 2011**,** **50**, 7879**.**
12 Wang, W.; Hong, Y.; Shi, X.; Minot, C.; Van Hove, M. A.; Tang, B. Z.; Lin, N. *J. Phys. Chem. Lett.* 2010, **1**, 2295.
13 Z. Shi and N. Lin, *J. Am. Chem. Soc.*, 2010, **132**, 10756.
14. Y. Li, J. Xiao, T. Shubina, M. Chen, Z. Shi, M. Schmid, H-P. Steinrueck, M. Gottfried, N. Lin, *J. Am. Chem. Soc*. 2012, **134**, 6401.